THE JOURNAL OF PHYSICAL CHEMISTRY Letters

Letter

Cite This: J. Phys. Chem. Lett. 2019, 10, 3536−3542

pubs.acs.org/JPCL

Vapor-Deposited Glass Structure Determined by Deposition Rate−Substrate Temperature Superposition Principle

Camille Bishop,*[,†] Ankit Gujral,[†] Michael F. Toney,[§] Lian Yu,[‡] and Mark D. Ediger[†]

[†]Department of Chemistry, University of Wisconsin—Madison, Madison, Wisconsin 53706, United States

[‡]School of Pharmacy, University of Wisconsin—Madison, Madison, Wisconsin 53706, United States

[§]Stanford Synchrotron Radiation Lightsource, SLAC National Accelerator Laboratory, Menlo Park, California 94025, United States

Supporting Information

ABSTRACT: We show that deposition rate substantially affects the anisotropic structure of thin glassy films produced by physical vapor deposition. Itraconazole, a glass-forming liquid crystal, was deposited at rates spanning 3 orders of magnitude over a 25 K range of substrate temperatures, and structure was characterized by ellipsometry and X-ray scattering. Both the molecular orientation and the spacing of the smectic layers obey deposition rate−substrate temperature superposition, such that lowering the deposition rate is equivalent to raising the substrate temperature. We identify two different surface relaxations that are responsible for structural order in the vapor-deposited glasses and find that the process controlling molecular orientation is accelerated by more than 3 orders of magnitude at the surface relative to the bulk. The identification of distinct surface processes responsible for anisotropic structural features in vapor-deposited glasses will enable more precise control over the structure of glassy materials used in organic electronics.

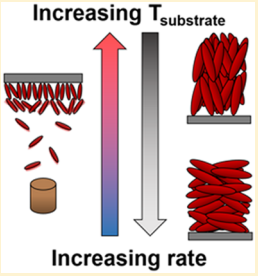

Vapor-deposited glasses of organic semiconductors are important materials used in organic electronics, such as organic light-emitting diodes (OLEDs). Compared to their liquid-cooled counterparts, vapor-deposited glasses can have much higher thermal stability[1,2] and can be anisotropic.[3] Structural anisotropy can impart extra functionality to these materials while preserving the homogeneity and compositional flexibility expected for amorphous materials. In OLEDs for example, the outcoupling efficiency can be significantly increased if the transition dipoles of emitter molecules lie in the plane of the substrate.[4−6] Even more highly structured amorphous thin films, such as those with liquid crystalline order,[7] may be useful for next-generation devices such as organic field effect transistors and photovoltaics.[8] While the control of thermal stability in vapor-deposited glasses is well understood,[1−3] we know considerably less about how deposition parameters influence structural anisotropy, particularly for highly anisotropic structures. In this work, we show that the anisotropic structure of a vapor-deposited glass can be significantly altered by varying the deposition rate. We find that for some glass properties raising the substrate temperature during deposition is equivalent to depositing more slowly, and we define a deposition rate−substrate temperature superposition. We determine the time scales of surface relaxations that are responsible for the structure in vapor-deposited glasses and find that they are significantly faster than those in the bulk glass.

Past work has shown that substrate temperature is an important parameter for determining the properties of vapor-deposited glasses. The proper choice of substrate temperature during physical vapor deposition can increase the thermal stability and density[1] of the resulting glass, leading to longer lifetimes when used in OLED devices.[9] Glasses with exceptional properties are typically produced when deposited onto substrates held at temperatures in the range $0.8-0.9T_g$, where T_g is the glass transition temperature. The unique properties of vapor-deposited glasses have been explained by a surface equilibration mechanism.[1,3] For this mechanism, enhanced mobility near the surface of the glass[10,11] allows substantial equilibration during deposition even though the temperature is below T_g.[1,3,12,13] When the substrate temperature is chosen optimally, equilibration during deposition is sufficient to produce a material with density and thermal stability that are considerably higher than those that can be achieved by liquid cooling.[1,3] The substrate temperature also influences the structural anisotropy of vapor-deposited glasses,[13] including the extent of molecular orientation,[3,14−16] creating glasses that may be impossible to attain by liquid cooling.[17]

In contrast to the substrate temperature, the influence of deposition rate on the properties of vapor-deposited glasses has been less explored. Lowering the deposition rate at constant substrate temperature has been observed to increase kinetic stability[18,19] until a limiting stability is achieved, as expected from the surface equilibration mechanism. There have been a few studies on the effect of deposition rate upon anisotropic structure in vapor-deposited glasses,[13,15,17,20,21] but it is difficult to synthesize a consistent viewpoint from this work. To our knowledge, only one study has addressed the influence of deposition rate on molecular orientation in vapor-deposited

Received: May 14, 2019
Accepted: June 9, 2019
Published: June 9, 2019

DOI: 10.1021/acs.jpclett.9b01377
J. Phys. Chem. Lett. 2019, 10, 3536−3542

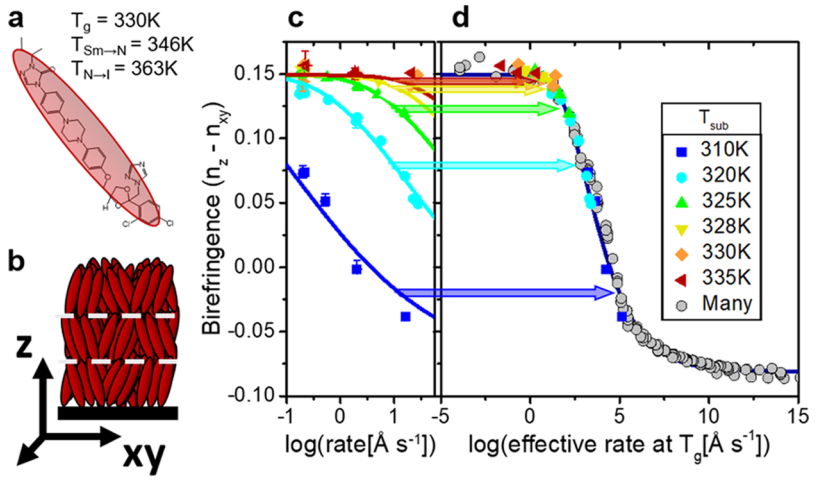

Figure 1. Illustration of the deposition rate−substrate temperature superposition for birefringence of itraconazole deposited at several rates and six substrate temperatures. (A) Molecular structure of itraconazole, represented as a rod, with phase transition temperatures. (B) Definition of film axes with respect to the substrate. (C) Birefringence, which correlates with molecular orientation, as a function of deposition rate at six substrate temperatures. (D) Data from previous panel shifted by 0.196 decades of deposition rate per K, the superposition shift factor. Gray data is previously published birefringence of samples deposited at 2 Å s^{-1} at many T_{sub} from Gómez et al.,[16] shifted by the same factor.

glasses, and it concluded that rate had little to no effect.[15] Two studies utilizing X-ray scattering have reported an effect of deposition rate upon anisotropic structure in vapor-deposited glasses. Bagchi et al. found a small shift in molecular layer spacing of Alq_3 deposited at two different rates,[13] while Dawson et al. found variable degrees of layering order from indomethacin deposited at various rates.[17,21] Although these last two studies show that deposition rate can influence the structure of a PVD glass, they do not provide clear guidelines for how to manipulate deposition rate to produce a desired structure.

In this work, we utilize a wide range of deposition rates and substrate temperatures to prepare glasses of itraconazole, a glass-forming smectic liquid crystal. We characterize the molecular orientation of the glasses by spectroscopic ellipsometry[16] and the anisotropic layering by grazing-incidence wide-angle X-ray scattering (GIWAXS).[22,23] Itraconazole is an ideal choice for these experiments as its liquid and liquid-cooled glass have been well-characterized.[24−27] Previous vapor deposition experiments have established that depositing at different substrate temperatures can prepare glasses of itraconazole with a wide range of molecular orientations, with some deposition conditions preparing glasses with high levels of smectic order. These features provide a rich set of observables for investigating the influence of deposition rate on glassy molecular packing.

We find that deposition rate has a very significant influence on the structure of vapor-deposited glasses of itraconazole. Depositions at T_g − 10 K, for example, produce glasses with a strong tendency for the molecular long axis to be oriented along the surface normal if the deposition rate is low, whereas nearly isotropic orientation is obtained at high deposition rates. Additionally, we find that the deposition rate and substrate temperature can be collapsed into a single variable that controls the structural features of the glass. We thus introduce a new principle for understanding the anisotropic structure of PVD glasses: deposition rate−substrate temperature superposition (RTS). RTS for PVD glasses is a nonequilibrium analogy to the equilibrium time−temperature superposition (TTS) that has been used extensively to investigate the dynamics of polymeric[28] and small-molecule[29,30] glasses. When a process follows RTS or TTS, a master curve can be generated (based upon a small set of experiments) that forecasts properties over a wide range of temperatures and rates. We anticipate that RTS will be a powerful tool for designing vapor-deposited glasses with particular anisotropic structures, both for molecules that have equilibrium liquid crystal phases and those that do not.

Itraconazole (structure shown Figure 1a) was vapor deposited at six substrate temperatures, using deposition rates spanning nearly 3 orders of magnitude. The molecular orientation of the vapor-deposited glasses was determined from birefringence, with the out-of-plane *z*-axis and in-plane *xy*-axes defined in Figure 1b. The birefringence is the difference in refractive indices out of and in the plane ($n_z - n_{xy}$) and is directly proportional to the average orientation of the long axes of the molecules.[16] A more positive value for birefringence corresponds to a more vertical orientation of the long axis of the molecules with respect to the substrate. The maximum birefringence attained in this work corresponds to an average angle of 27° between the long axes of the molecules and the substrate normal; the minimum birefringence corresponds to an angle of 79°.

The deposition rate significantly alters the molecular orientation of itraconazole, with glasses deposited more slowly having a higher birefringence (more vertical molecular orientation) at all substrate temperatures (Figure 1c). For example, at $T_{substrate}$ = 310 K, depositing at rates that cover nearly 3 orders of magnitude produces glasses for which the birefringence varies by more than 0.1. Over this range, the average angle of the molecules with respect to the surface normal varies from 65° for the fastest deposition to 42° for the slowest. As shown in previous work[16] in which the deposition rate was held constant, increasing the substrate temperature also results in higher birefringence. Curves shown in Figure 1c are Kohlrausch−Williams−Watts (KWW) fits to the data and will be addressed in more detail in Figure 4.

The two parameters of deposition rate and substrate temperature can be collapsed into a single variable by defining a deposition rate−substrate temperature superposition for

DOI: 10.1021/acs.jpclett.9b01377
J. Phys. Chem. Lett. 2019, 10, 3536−3542

birefringence. The RTS, shown in Figure 1d, is created by horizontally shifting the single-substrate temperature curves shown in Figure 1c on the log scale. We define an effective deposition rate at T_g, i.e., the rate at which itraconazole would need to be deposited at 330 K to attain a given birefringence, that relates the effective and actual rates as shown in eq 1:

$$R_{\text{eff}} = R_{\text{actual}} \frac{\tau(T_{\text{sub}})}{\tau(T_g)} \tag{1}$$

$\tau(T_{\text{sub}})/\tau(T_g)$ is the ratio of the interfacial relaxation time at a given substrate temperature to that at T_g. For vapor-deposited itraconazole, eq 1 is satisfied when $\log(\tau(T_{\text{sub}})/\tau(T_g))$ is equal to $(0.196\ \text{K}^{-1})(T_g - T_{\text{sub}})$. The resulting "shift factor" of 0.196 decades per Kelvin determines the amount by which each curve shifts between panels c and d of Figure 1.

Over this wide range of deposition temperatures and rates, raising the substrate temperature by 1 K is equivalent to depositing 1.6 times more slowly. Along with data from this work, we show previously published birefringence data by Gómez et al.[16] for glasses deposited at a wide range of substrate temperatures and a single deposition rate (2 Å s^{-1}). When these substrate temperatures are converted to the effective rate by using eq 1, they follow the master curve produced by this work and predict the results from a much larger set of experimental conditions.

Next, we use grazing incidence wide-angle X-ray scattering (GIWAXS) to determine if the molecular packing of vapor-deposited glasses of itraconazole is similarly consistent with RTS. Sample two-dimensional GIWAXS patterns are shown in Figure 2. Two main structural features appear. The scattering

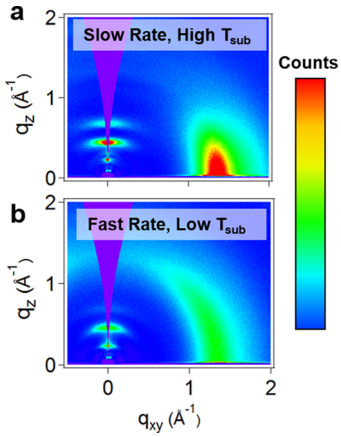

Figure 2. Grazing incidence wide-angle X-ray scattering (GIWAXS) of vapor-deposited itraconazole with high and low levels of smectic order. (A) Itraconazole vapor deposited at T_{sub} = 335 K, 0.2 Å s^{-1} and (B) T_{sub} = 320 K, 26 Å s^{-1}. Both GIWAXS patterns are from 400 nm films exposed for 120 s at an incidence angle of θ_{in} = 0.14°. Counts are shown on a linear scale.

at $q \approx 1.4$ Å^{-1} corresponds to the distance of closest approach between neighboring rods. The distribution of intensity of this broad feature along the radial direction provides information about orientational order in the glass.[22,31] The diffraction features at $q_z \approx 0.2$, 0.4, and 0.6 Å^{-1} provide information about the positional smectic-like packing[22,32] associated with the layering of the molecules. The position of these peaks (along q_z) shows that the layers are parallel to the substrate, as illustrated in Figure 1b. We note that for the glass deposited more slowly at the higher substrate temperature (Figure 2a), the peaks along q_z are sharper, and the scattering at $q \approx 1.4$ Å^{-1} is more localized, indicating a higher degree of smectic order than for the glass shown in Figure 2b.

We investigate whether the positional order in vapor-deposited itraconazole glasses can also be described by RTS. Previous work has shown that the period of the layer spacing, as determined from the peak position along q_z, can be selected by choosing the substrate temperature.[22] To investigate possible RTS for the layering spacing in these samples, GIWAXS was done at the local specular condition[33] to provide full resolution of the second-order smectic layering peak in itraconazole glasses. The second-order peak is chosen, rather than the first, to avoid interference from background scattering. The resulting 2D diffraction patterns of the second-order peaks are shown in Figure 3. Integrations along the azimuthal direction over an 80° range of angles are shown in Figure 3c. We quantify the peak position, as it is an unambiguous measure of spacing between smectic layers.[25] For the sample deposited at 335 K, the second-order peak occurs at smaller q, indicating increased spacing between smectic layers. The peak positions in q are plotted against deposition rate in Figure 3d. For a given substrate temperature, depositing more slowly results in a glass with smaller q-spacing, which corresponds to an increase in smectic layer spacing. The peak positions found in this work correspond to a range of real-space periodicities from 26.2 to 29.9 Å, a 14% change in layer spacing.

As with birefringence, the smectic spacing obeys an RTS that collapses deposition rate and substrate temperature into a single variable, shown in Figure 3e. The shift factor for the layer spacing is 0.47 decades per K, found by fitting the data to a polynomial curve and minimizing error (fitting procedure in SI section 1). Using this shift factor, we define an effective deposition rate at T_g which corresponds to the deposition rate needed to achieve a given layer spacing for a substrate temperature of 330 K. Similarly to Figure 1d, variable substrate temperature data from samples deposited at 2 Å s^{-1} have been replotted from Gujral et al.[22] after converting to the new effective rate using eq 1 with the new shift factor of 0.47 decades K^{-1}. Good agreement is observed between the data presented here (exploring deposition rate and substrate temperature) and the previously published results (exploring only substrate temperature, but over a larger range). We have confirmed the uniqueness of the shift factors, as demonstrated in SI Figure 4.

The existence of the RTS found in this work can be explained by the surface equilibration mechanism, which rationalizes the properties of vapor-deposited glasses.[1,12,13] Molecules near the free surface of an organic glass have much higher mobility than molecules in the bulk.[10,11] During deposition, molecules near the surface can sample different packing arrangements and move toward equilibrium before becoming trapped in the bulk by further deposition. Previous work has shown that depositing at lower rates (i.e., giving the molecules more time to equilibrate) results in glasses with greater kinetic stability.[18,19] Here we show that depositing at lower rates also allows more time to achieve the structure preferred at the free surface (nearly vertical molecules in smectic layers parallel to the surface). Furthermore, raising the temperature is shown to have the same effect as depositing more slowly; higher surface mobility at the higher temperature allows a given amount of equilibration to be achieved more quickly. We therefore understand RTS as a kinetic

DOI: 10.1021/acs.jpclett.9b01377
J. Phys. Chem. Lett. 2019, 10, 3536−3542

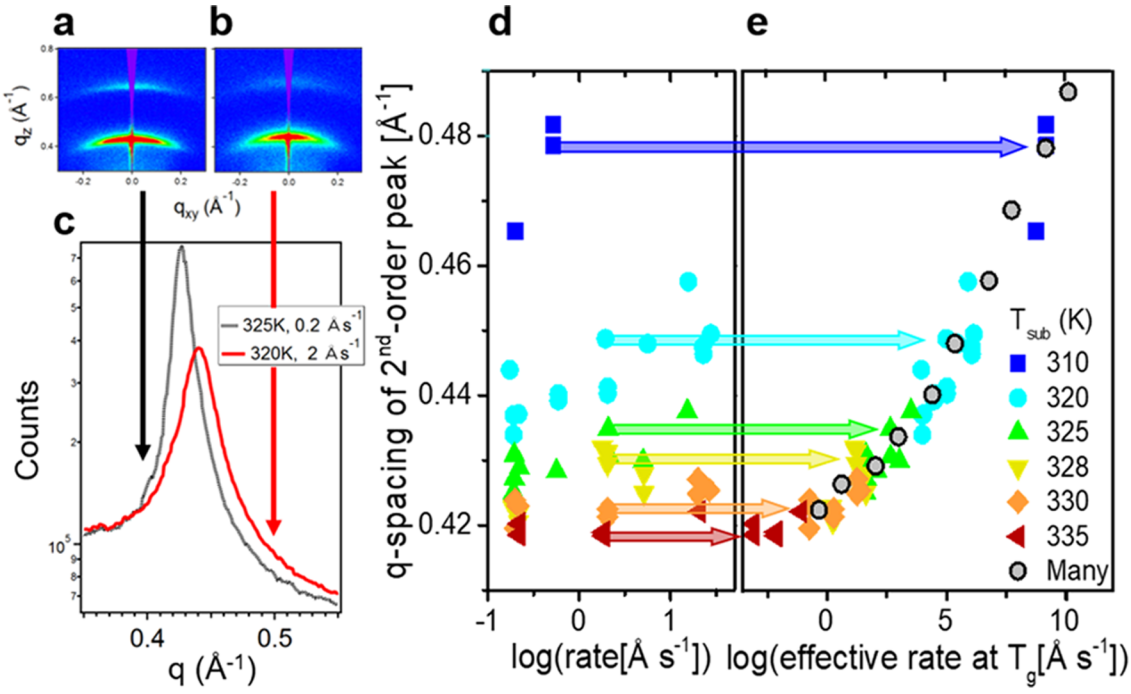

Figure 3. Illustration of RTS for the q-value associated with smectic layer spacing of vapor-deposited itraconazole. (A and B) GIWAXS at the local specular condition for the second-order q_z diffraction peak for itraconazole vapor deposited at T_{sub} = 325 K, 0.2 Å s^{-1} and T_{sub} = 320 K, 2 Å s^{-1}, respectively. (C) Azimuthal integrations of scattering in panels A and B as a function of q. (D) q-spacing of second-order diffraction peak as a function of deposition rate. (E) Successful RTS of data from panel D using a shift factor of 0.47 decades of deposition rate per K. Gray data is previously published peak positions of samples deposited at 2 Å s^{-1} from Gujral et al.,[22] shifted by the same factor.

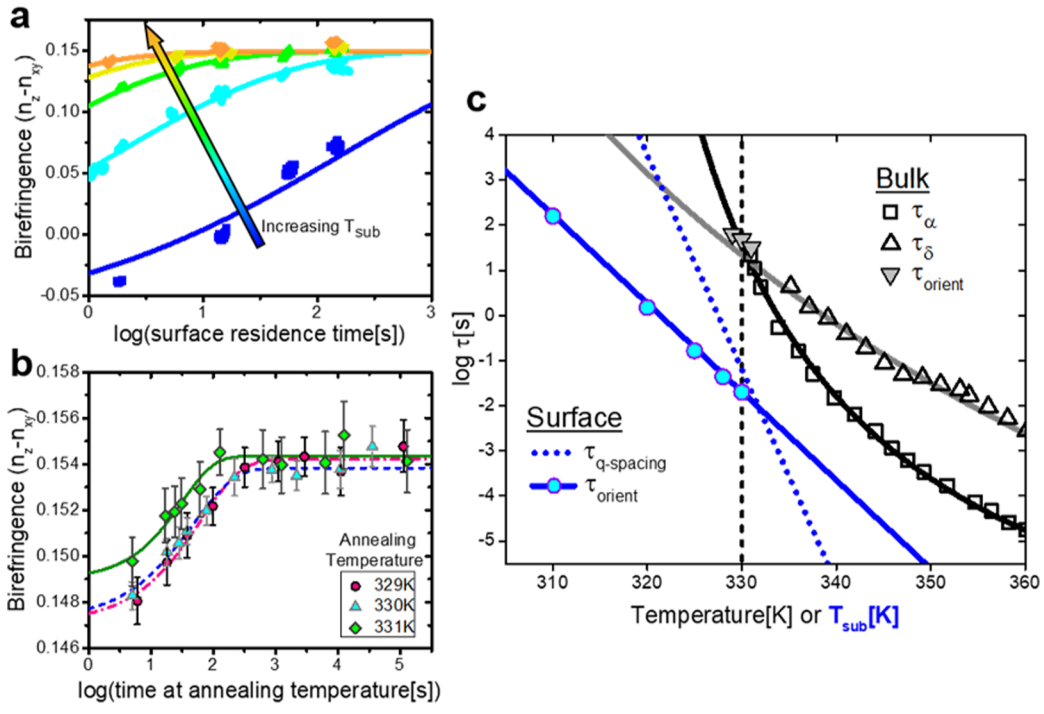

Figure 4. Surface and bulk relaxation processes for itraconazole. (A) Birefringence data from Figure 1c with deposition rate converted to surface residence time, fit to the KWW function with β = 0.28. (B) Birefringence versus annealing time for bulk films after a jump down in temperature, with KWW fits. (C) Relaxation time plot for itraconazole, with bulk processes shown in grayscale and surface processes shown in blue. Hollow symbols are from dielectric experiments of Tarnacka et al.,[26] with lines representing VFT fits. Filled circles and downward pointing triangles are τ values from KWW fits to data in panels a and b, respectively. Solid and dashed blue lines represent temperature dependences of the surface relaxation processes.

phenomenon and expect it to hold when the equilibrium structure is not a strong function of temperature.

We can determine the relaxation times of the surface processes responsible for anisotropic structural order in the

DOI: 10.1021/acs.jpclett.9b01377
J. Phys. Chem. Lett. 2019, 10, 3536−3542

PVD glass by utilizing our variable rate and temperature data. To do this, we fit birefringence as a function of deposition rate to KWW functions (Figure 4a) to find a surface relaxation time at each temperature. We use a fitting procedure similar to that used by Chua et al.[18] By assuming a 30 Å mobile layer at the surface, we define the average surface residence time as follows:

$$t = \frac{30\ \text{Å}}{\text{deposition rate } (\text{Å s}^{-1})} \tag{2}$$

Here, we choose 30 Å as the mobile layer depth because it is roughly the length of one molecule. As shown in Figure 4a, as the molecules spend more time at the surface, more birefringent glasses result; this occurs because the molecules have more time at the free surface to become vertically oriented before becoming trapped by further deposition. We fit the data in Figure 4a to a stretched exponential of the form

$$(n_z - n_{xy}) = A \exp\left(-\left(\frac{t}{\tau}\right)^{\beta}\right) + C \tag{3}$$

where t is the free surface residence time and τ is the surface relaxation time. (Details of the fitting procedure are given in SI section 2). From this procedure, we infer the relaxation time for molecular orientation at the surface of itraconazole. The distinct shift factors for the birefringence (Figure 1) and q-spacing (Figure 3) lead us to identify two distinct surface relaxation processes that determine these structural features.

Consistent with the surface equilibration mechanism, we find that the relaxation time associated with molecular orientation is much faster at the surface than in the bulk. As eq 1 demonstrates, the relaxation time at the surface determines the effective deposition rate conversion factor for a given system. We determine the surface relaxation time for orientation as described in the previous paragraph; these data are plotted in Figure 4c as cyan circles. To determine the corresponding relaxation time for molecular orientation in the bulk, we measured the birefringence of films of itraconazole rapidly quenched from T_g + 14 K as a function of annealing time at three temperatures; this data shown in Figure 4b was fit to eq 3 and provides the bulk orientation times shown as colored triangles in Figure 4c. Figure 4c indicates that molecular reorientation is more than 3 orders of magnitude faster at the surface than in the bulk. Tarnacka et al. have reported two (bulk) relaxation modes (α and δ) for itraconazole by dielectric spectroscopy,[26] and these are shown in Figure 4c with corresponding VFT fits (fitting details shown SI section 3). The bulk δ mode is thought to correspond to the end-over-end rotation of the molecule about its short axis[26,27] and, by extrapolation, agrees with the orientation relaxation times for the bulk determined here.

Figure 4c also shows the surface relaxation time associated with the development of smectic layer distance $\tau_{q\text{-spacing}}$ obtained from an analysis of the data in Figure 3. The temperature dependence of this process is set by the observed shift factor. While there is uncertainty in the absolute relaxation time for this process, we estimate that it is half an order of magnitude slower than the relaxation of molecular orientation at the surface at T_g (more information in SI section 4.) It is known that multiple relaxation processes with different temperature dependences exist for bulk glassformers, e.g., structural relaxation and self-diffusion.[34,35] It is certainly reasonable that there are multiple relaxation processes at the surface of a glass as well, and previous work provides some support for this.[36,37] As the surface diffusion coefficient of itraconazole has not yet been measured, it is not known how the two surface relaxation times characterized here might be connected with surface diffusion.

The molecular origin of the two surface relaxation processes of itraconazole is an important question, and we speculate that they are related to the two relaxation modes of the bulk supercooled liquid. The work of Tarnacka et al.[26] identifies two bulk relaxation modes from dielectric measurements: the α mode, which is related to the calorimetric glass transition, and the δ mode, which is determined by reorientation of the long axis of the itraconazole molecule. The ratio of the apparent activation energies of $\tau_{q\text{-spacing}}$ to τ_{orient} is equal to the ratio of the apparent activation energies of τ_α to τ_δ, suggesting a correspondence between bulk and surface modes. It is certainly reasonable that τ_{orient} is connected with τ_δ, as both involve reorientation of the long axis of the molecule. Many glass-forming systems do not show distinct α and δ modes in the bulk, and it is possible that these systems will obey RTS with only a single shift factor; it is likely that the numerical value of the shift factor will be different for different systems.

RTS provides a clear framework for understanding the few previous efforts to understand the impact of deposition rate on the structure of vapor-deposited glasses. In the most relevant work, Yokoyama[15] found that rate had little to no effect on molecular orientation in vapor-deposited glasses of several organic electronics molecules. Using RTS, we can understand this result as the experiments were done at low substrate temperatures ($0.71-0.77T_g$). For itraconazole, Yokoyama's deposition conditions would correspond to an effective deposition rate at T_g of nearly 10^{15} Å s^{-1}. As can be seen in Figure 1d, this rate is so high that no discernible effect is expected when changing the deposition rate by 2 orders of magnitude. Two studies have used X-ray scattering to address the effect of deposition rate on anisotropic layering in vapor-deposited glasses. Bagchi et al. found the molecular layer spacing in vapor-deposited Alq_3 changed by a small amount with a 7-fold change in deposition rate; the observed trend is consistent with RTS.[13] Dawson et al. studied the degree of order in vapor-deposited indomethacin from the intensity of an anisotropic layering peak.[17] In the range from 0.94 to $1.0T_g$, which is the range studied for itraconazole in the current work, Dawson et. al's data is consistent with RTS within error. In the lower substrate temperature regime, the data does not superimpose, suggesting the importance of additional factors beyond those considered here.

In summary, we find that deposition rate can significantly affect the structure of a vapor-deposited glass; this result is consistent with the surface equilibration mechanism that has been proposed to account for the kinetic stability of vapor-deposited glasses. For itraconazole, the combined effect of substrate temperature and deposition rate on important structural features can be described by a superposition principle. For properties which are described by RTS, multiple sets of deposition conditions can be used to produce the same features. For example, to deposit a film with desired structure faster, the substrate temperature can be raised to compensate for lack of equilibration time. In cases where the substrate temperature cannot be changed, the desired structure can be achieved by adjusting the deposition rate. We expect that RTS will facilitate predictive engineering of vapor-deposited glasses of both liquid crystal and non-liquid crystal systems.

DOI: 10.1021/acs.jpclett.9b01377
J. Phys. Chem. Lett. 2019, 10, 3536−3542

Additionally, RTS allows an estimate of surface relaxation times for organic glasses. For itraconazole at T_g, the relaxation process governing molecular orientation is approximately three and a half orders of magnitude faster at the surface than in the bulk.

EXPERIMENTAL METHODS

Samples were prepared by thermal evaporation on Si ⟨100⟩ wafers with 2 nm of native oxide (Virginia Semiconductor) in a home-built high-vacuum chamber at a pressure of 10^{-6} Torr as detailed in prior publications.[16] Deposition rate was monitored by a quartz crystal microbalance (Sycon). Within each deposition, the rate varied by no more than 10%; the true average deposition rate was calculated from the ellipsometrically determined film thickness. Substrate temperature was controlled with Lakeshore 336 and 340 temperature controllers.

As-deposited films were characterized using a J.A. Woollam M-2000U variable angle spectroscopic ellipsometer. Each wafer of a single substrate temperature was measured at 21 points with 7 angles. Optical constants were determined by fitting data at wavelengths between 500 and 1000 nm to a uniaxially anisotropic Cauchy model in which the two optical axes, the ordinary and extraordinary, are described by

$$n_o = A_o + \frac{B}{\lambda^2},\ n_e = A_e + \frac{B}{\lambda^2} \tag{4}$$

Each sample was approximately 400 nm thick, with an overall thickness gradient of ∼15% across the 1 in. wafer. This results in a spread of deposition rates and birefringences across each sample. Each data point in Figure 1 represents a single wafer, with bars indicating the overall range of rates and birefringences if larger than the symbol size.

X-ray scattering was performed with both a synchrotron and a lab source. Q-spacings for the two instruments are presented without distinction in this work; on both instruments, data was acquired at the local specular condition for the second-order peak. For the GIWAXS data in Figure 2, the incidence angle was $\theta_{in} = 0.14°$.

Synchrotron data was taken on Beamline 11-3 at the Stanford Synchrotron Radiation Lightsource, equipped with a two-dimensional Rayonix MX255 CCD area detector. The sample-to-detector distance was 315 mm, and the wavelength of radiation was 0.973 Å. Samples were exposed for 120 s. Data was reduced using the WAXStools Macro[38] in the Nika data reduction package for Igor Pro.[39,40] Lab source data was acquired with a Bruker D8 Discovery Diffractometer with a Cu Kα X-ray source with wavelength of 1.54 Å, equipped with a VANTEC500 area detector. The spot size was 2 mm, and samples were exposed for 240 s.

ASSOCIATED CONTENT

Supporting Information

The Supporting Information is available free of charge on the ACS Publications website at DOI: 10.1021/acs.jpclett.9b01377.

Determination of shift factors (SI Figures 1−3), uniqueness of shift factors (SI Figures 4 and 5), stretched exponential fitting of birefringence data (SI Figures 6 and 7), VFT fitting in Figure 4 (SI Table 1 and SI Figure 8), determination of surface relaxation time for smectic q-spacing (SI Figures 9 and 10) (PDF)

AUTHOR INFORMATION

Corresponding Author

*Phone: 608-262-5547. E-mail: cbishop4@wisc.edu.

ORCID

Camille Bishop: 0000-0002-2889-1752
Ankit Gujral: 0000-0002-5065-2694
Michael F. Toney: 0000-0002-7513-1166
Lian Yu: 0000-0002-4253-5658
Mark D. Ediger: 0000-0003-4715-8473

Notes

The authors declare no competing financial interest.

ACKNOWLEDGMENTS

This research was primarily supported by NSF through the University of Wisconsin Materials Research Science and Engineering Center (DMR-1720415). Use of the Stanford Synchrotron Radiation Lightsource, SLAC National Accelerator Laboratory, is supported by the U.S. Department of Energy, Office of Science, Office of Basic Energy Sciences under Contract No. DE-AC02-76SF00515. We thank Tim Dunn and Chris Tassone for assistance on Beamline 11-3.

REFERENCES

(1) Swallen, S. F.; Kearns, K. L.; Mapes, M. K.; Kim, Y. S.; McMahon, R. J.; Ediger, M. D.; Wu, T.; Yu, L.; Satija, S. Organic Glasses with Exceptional Thermodynamic and Kinetic Stability. *Science* **2007**, *315*, 353−356.

(2) Rodríguez-Tinoco, C.; Gonzalez-Silveira, M.; Ràfols-Ribé, J.; Lopeandía, A. F.; Rodríguez-Viejo, J. Transformation kinetics of vapor-deposited thin film organic glasses: the role of stability and molecular packing anisotropy. *Phys. Chem. Chem. Phys.* **2015**, *17*, 31195−31201.

(3) Dalal, S. S.; Walters, D. M.; Lyubimov, I.; de Pablo, J. J.; Ediger, M. D. Tunable molecular orientation and elevated thermal stability of vapor-deposited organic semiconductors. *Proc. Natl. Acad. Sci. U. S. A.* **2015**, *112*, 4227−4232.

(4) Komino, T.; Tanaka, H.; Adachi, C. Selectively Controlled Orientational Order in Linear-Shaped Thermally Activated Delayed Fluorescent Dopants. *Chem. Mater.* **2014**, *26*, 3665−3671.

(5) Schmidt, T. D.; Lampe, T.; Sylvinson, D.; Djurovich, P. I.; Thompson, M. E.; Brütting, W. Emitter Orientation as a Key Parameter in Organic Light-Emitting Diodes. *Phys. Rev. Appl.* **2017**, *8*, 037001.

(6) Frischeisen, J.; Yokoyama, D.; Adachi, C.; Brütting, W. Determination of molecular dipole orientation in doped fluorescent organic thin films by photoluminescence measurements. *Appl. Phys. Lett.* **2010**, *96*, 073302.

(7) Suga, H.; Seki, S. Thermodynamic investigation on glassy states of pure simple compounds. *J. Non-Cryst. Solids* **1974**, *16*, 171−194.

(8) O'Neill, M.; Kelly, S. M. Ordered materials for organic electronics and photonics. *Adv. Mater.* **2011**, *23*, 566−584.

(9) Ràfols-Ribé, J.; Will, P.-A.; Hänisch, C.; Gonzalez-Silveira, M.; Lenk, S.; Rodríguez-Viejo, J.; Reineke, S. High-performance organic light-emitting diodes comprising ultrastable glass layers. *Sci. Adv.* **2018**, *4*, No. eaar8332.

(10) Brian, C. W.; Yu, L. Surface Self-Diffusion of Organic Glasses. *J. Phys. Chem. A* **2013**, *117*, 13303−13309.

(11) Yu, L. Surface mobility of molecular glasses and its importance in physical stability. *Adv. Drug Delivery Rev.* **2016**, *100*, 3−9.

(12) Lyubimov, I.; Antony, L.; Walters, D. M.; Rodney, D.; Ediger, M. D.; de Pablo, J. J. Orientational anisotropy in simulated vapor-deposited molecular glasses. *J. Chem. Phys.* **2015**, *143*, 094502.

(13) Bagchi, K.; Jackson, N. E.; Gujral, A.; Huang, C.; Toney, M. F.; Yu, L.; de Pablo, J. J.; Ediger, M. D. Origin of Anisotropic Molecular

DOI: 10.1021/acs.jpclett.9b01377
J. Phys. Chem. Lett. 2019, 10, 3536−3542

Packing in Vapor-Deposited Alq3 Glasses. *J. Phys. Chem. Lett.* **2019**, *10*, 164−170.
(14) Lin, H.-W.; Lin, C.-L.; Chang, H.-H.; Lin, Y.-T.; Wu, C.-C.; Chen, Y.-M.; Chen, R.-T.; Chien, Y.-Y.; Wong, K.-T. Anisotropic optical properties and molecular orientation in vacuum-deposited ter(9,9-diarylfluorene)s thin films using spectroscopic ellipsometry. *J. Appl. Phys.* **2004**, *95*, 881−886.
(15) Yokoyama, D. Molecular orientation in small-molecule organic light-emitting diodes. *J. Mater. Chem.* **2011**, *21*, 19187−19202.
(16) Gómez, J.; Jiang, J.; Gujral, A.; Huang, C.; Yu, L.; Ediger, M. D. Vapor deposition of a smectic liquid crystal: highly anisotropic, homogeneous glasses with tunable molecular orientation. *Soft Matter* **2016**, *12*, 2942−2947.
(17) Dawson, K. J.; Zhu, L.; Yu, L.; Ediger, M. D. Anisotropic structure and transformation kinetics of vapor-deposited indomethacin glasses. *J. Phys. Chem. B* **2011**, *115*, 455−463.
(18) Chua, Y. Z.; Ahrenberg, M.; Tylinski, M.; Ediger, M. D.; Schick, C. How much time is needed to form a kinetically stable glass? AC calorimetric study of vapor-deposited glasses of ethylcyclohexane. *J. Chem. Phys.* **2015**, *142*, 054506.
(19) Kearns, K. L.; Krzyskowski, P.; Devereaux, Z. Using deposition rate to increase the thermal and kinetic stability of vapor-deposited hole transport layer glasses via a simple sublimation apparatus. *J. Chem. Phys.* **2017**, *146*, 203328.
(20) Hellman, F. Surface-induced ordering: A model for vapor-deposition growth of amorphous materials. *Appl. Phys. Lett.* **1994**, *64*, 1947−1949.
(21) Dawson, K. J.; Kearns, K. L.; Yu, L.; Steffen, W.; Ediger, M. D. Physical vapor deposition as a route to hidden amorphous states. *Proc. Natl. Acad. Sci. U. S. A.* **2009**, *106*, 15165−15170.
(22) Gujral, A.; Gómez, J.; Jiang, J.; Huang, C.; O'Hara, K. A.; Toney, M. F.; Chabinyc, M. L.; Yu, L.; Ediger, M. D. Highly Organized Smectic-like Packing in Vapor-Deposited Glasses of a Liquid Crystal. *Chem. Mater.* **2017**, *29*, 849−858.
(23) Rivnay, J.; Mannsfeld, S. C. B.; Miller, C. E.; Salleo, A.; Toney, M. F. Quantitative Determination of Organic Semiconductor Microstructure from the Molecular to Device Scale. *Chem. Rev.* **2012**, *112*, 5488−5519.
(24) Six, K.; Verreck, G.; Peeters, J.; Binnemans, K.; Berghmans, H.; Augustijns, P.; Kinget, R.; Van den Mooter, G. Investigation of thermal properties of glassy itraconazole: identification of a monotropic mesophase. *Thermochim. Acta* **2001**, *376*, 175−181.
(25) Benmore, C. J.; Mou, Q.; Benmore, K. J.; Robinson, D. S.; Neuefeind, J.; Ilavsky, J.; Byrn, S. R.; Yarger, J. L. A SAXS-WAXS study of the endothermic transitions in amorphous or supercooled liquid itraconazole. *Thermochim. Acta* **2016**, *644*, 1−5.
(26) Tarnacka, M.; Adrjanowicz, K.; Kaminska, E.; Kaminski, K.; Grzybowska, K.; Kolodziejczyk, K.; Wlodarczyk, P.; Hawelek, L.; Garbacz, G.; Kocot, A.; Paluch, M. Molecular dynamics of itraconazole at ambient and high pressure. *Phys. Chem. Chem. Phys.* **2013**, *15*, 20742.
(27) Teerakapibal, R.; Huang, C.; Gujral, A.; Ediger, M. D.; Yu, L. Organic Glasses with Tunable Liquid-Crystalline Order. *Phys. Rev. Lett.* **2018**, *120*, 055502.
(28) Dannhauser, W.; Child, W. C.; Ferry, J. D. Dynamic Mechanical Properties of Poly-n-octyl methacrylate. *J. Colloid Sci.* **1958**, *13*, 103−113.
(29) Richert, R.; Duvvuri, K.; Duong, L. T. Dynamics of glass-forming liquids. VII. Dielectric relaxation of supercooled tris-naphthylbenzene, squalane, and decahydroisoquinoline. *J. Chem. Phys.* **2003**, *118*, 1828−1836.
(30) Olsen, N. B.; Christensen, T.; Dyre, J. C. Time-Temperature Superposition in Viscous Liquids. *Phys. Rev. Lett.* **2001**, *86*, 1271−1274.
(31) Gujral, A.; O'Hara, K. A.; Toney, M. F.; Chabinyc, M. L.; Ediger, M. D. Structural characterization of vapor-deposited glasses of an organic hole transport material with X-ray scattering. *Chem. Mater.* **2015**, *27*, 3341−3348.
(32) Seddon, J. M. Structural Studies of Liquid Crystals by X-ray Diffraction. In *Handbook of Liquid Crystals*; D. Demus, J. G., Gray, G.W., Spiess, H.-W., Vill, V., Eds.; Wiley-VCH: Weinheim, Germany, 1998; Vol. *1*, pp 635−679.
(33) Baker, J. L.; Jimison, L. H.; Mannsfeld, S.; Volkman, S.; Yin, S.; Subramanian, V.; Salleo, A.; Alivisatos, A. P.; Toney, M. F. Quantification of Thin Film Crystallographic Orientation Using X-ray Diffraction with an Area Detector. *Langmuir* **2010**, *26*, 9146−9151.
(34) Ngai, K. L.; Paluch, M. Classification of secondary relaxation in glass-formers based on dynamic properties. *J. Chem. Phys.* **2004**, *120*, 857−873.
(35) Swallen, S. F.; Ediger, M. D. Self-diffusion of the amorphous pharmaceutical indomethacin near Tg. *Soft Matter* **2011**, *7*, 10339−10344.
(36) Chen, Y.; Chen, Z.; Tylinski, M.; Ediger, M. D.; Yu, L. Effect of molecular size and hydrogen bonding on three surface-facilitated processes in molecular glasses: Surface diffusion, surface crystal growth, and formation of stable glasses by vapor deposition. *J. Chem. Phys.* **2019**, *150*, 024502.
(37) Zhang, Y.; Fakhraai, Z. Decoupling of surface diffusion and relaxation dynamics of molecular glasses. *Proc. Natl. Acad. Sci. U. S. A.* **2017**, *114*, 4915.
(38) Oosterhout, S. D.; Savikhin, V.; Zhang, J.; Zhang, Y.; Burgers, M. A.; Marder, S. R.; Bazan, G. C.; Toney, M. F. Mixing Behavior in Small Molecule:Fullerene Organic Photovoltaics. *Chem. Mater.* **2017**, *29*, 3062−3069.
(39) Zhang, F.; Ilavsky, J.; Long, G. G.; Quintana, J. P. G.; Allen, A. J.; Jemian, P. R. Glassy Carbon as an Absolute Intensity Calibration Standard for Small-Angle Scattering. *Metall. Mater. Trans. A* **2010**, *41*, 1151−1158.
(40) Ilavsky, J. Nika: software for two-dimensional data reduction. *J. Appl. Crystallogr.* **2012**, *45*, 324−328.

DOI: 10.1021/acs.jpclett.9b01377
J. Phys. Chem. Lett. 2019, 10, 3536−3542